Major findings in the third year of the project were in the following areas

1. **Evaluating the properties of data assimilation problem using MCMC inversion with 1D cloud resolving model and radar reflectivity observations**

As explained in the section on major activities we have implemented a 1D lagrangian cloud resolving model with MCMC (Markov Chain Monte Carlo) data assimilation algorithm (Posselt and Vukicevic, 2010) in order to evaluate properties of the radar reflectivity data assimilation problem with respect to the parameterized microphysical processes in terms of favorable conditions that would render the data assimilation problem better constrained and the solutions more accurate when using the data assimilation technique such as 4DVAR (or EnKF, for that matter). A progression of the nonlinear data assimilation problem toward well constrained formulation under varying conditions in the model and observations could be investigated thoroughly only by analysis of the full posterior pdf solutions as shown in Posselt and Vukicevic (2010). Motivated by this approach, in the second year the new activity was started involving the implementation of the 1D model and MCMC algorithm at UM by graduate student van Lier-Walqui and diagnostic analysis of the microphysical processes in the model and simulation of the reflectivity from this model solutions. In the third year large number of experiments were conducted with MCMC algorithm and 1D model in the study on characterizing properties of the microphysical parameterization and the related data assimilation problem. The study results are presented in new manuscript submitted for review and publication in Monthly Weather Review ("Quantifcation of Cloud Microphysical Parameterization Uncertainty using Radar Reflectivity", Van Lier-Walqui, Vukicevic and Posselt, 2011). In he following, the methodology and major findings of the study are summarized. The brief summary of the methodology is included in this section of the report on major findings to aid in better understanding of the study conclusions in section (1b).

1a) Brief description of methodology

The 1D lagrangian cloud model and the MCMC algorithm are described in detail in Posselt and Vukicevic (2010). Only brief summary is presented here. The model is designed to emulate the changes in environment experienced by an atmospheric column as it moves through a cloud system following the mean flow. The vertical profiles of temperature and moisture are fixed and the model is driven by specified time-varying vertical profiles of vertical motion and water vapor tendency. Advection is only allowed to operate on cloud liquid and ice condensate, and only in the vertical direction. By varying the vertical profiles of temperature, moisture, vertical motion, and water vapor forcing, the model can be adapted to simulate the flow through a range of different cloud systems. Since organized deep convection produces the bulk of the warm season precipitation globally, (and over the Great Plains in USA) and has been shown to be highly

sensitive to changes in cloud microphysical parameters, an idealized representation of squall line type convection is simulated by the model. The added benefit to examination of squall-line type convection is that it contains two discrete cloud morphologies; convective, in which precipitation is primarily generated by the collision-coalescence (warm rain) process, and stratiform, in which the melting of snow and graupel play a key role. The model is run with 60 vertical layers with constant 250 meter vertical grid spacing and a 5 second timestep, and the radiative transfer, surface flux, and microphysical parameterizations are all identical to those used in the the NASA Goddard Cumulus Ensemble Model (Tao and Simpson 1993, Tao et al. 2003, Lang et al. 2007). Time series of rain from the model solution over 60 min is shown in Figs. 10 (equivalent to Figure 2a in Posselt and Vukicevic). It can be seen that the model produces realistic time-evolution of a squall-line with the convective phase followed by the stratiform phase.

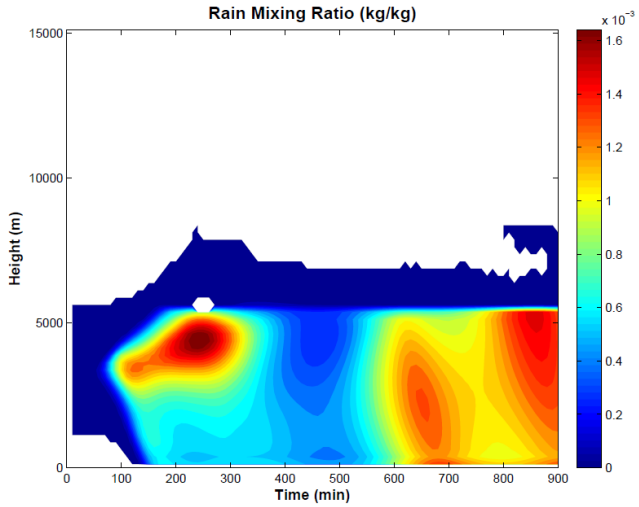

Figure 1: 1D Lagrangian model simulation of rain mixing ratio (kg/kg)

The project report in 2010 included the results from initial analysis of the model performance in the microphysical fields and illustration of the diagnostics that would be used in further analysis and data assimilation with the MCMC system. In the initial analysis we used Simulation of reflectivity and polarimetric differential reflectivity (SimPolRad) model to simulate reflectivity data to use in the data assimilation experiments. Although, the results using this radar-reflecivity model were satisfactory in terms of producing realistic reflecivity fields it was found, as noed in the last year project report, that the software was computationally inefficient for use in the data assimilation. We have investigated several options toward

improving the efficiency of SimPolRad but none have shown sufficient reduction in computing time to render feasible application with MCMC data assimilation algorithm, which by design requires millions of model simulations. We replaced SimPolRad with Quickbeam radar forward operator (Haynes et al. 2007) for a 3 GHz radar frequency (comparable to WSR-88D radar frequency). This new operator produced very similar radar reflectivity simulations to SimPolRad but with significantly higher efficiency. Quickbeam is capable of solving Mie equations for a variety of radar frequencies and a variety of user-specified particle size distributions and microphysical parameter values. In contrast to the work of Tong and Xue (2008), the perturbed values of the microphysical parameters are used in the radar forward operator. In this sense, the cloud microphysics model and the radar forward operator can be thought of as constituting a single, consistent forward model. In tests (not shown here), Quickbeam was found to be also comparable to other available forward operators such as SDSU (Masunaga et al. 2010) in relative distribution of reflectivity, with the exception of the melting layer reflectivity bright-band, which Quickbeam is unable to reproduce. Radar reflectivity is simulated at model grid resolution and beam bending, broadening and attenuation are not considered due to the idealized nature of the investigation. From this solution measurements are selected from two distinct storm morphological regimes: convective at 60 minutes and stratiform at 120 minutes.

In MCMC experiments ten microphysical parameters are chosen for their importance within the equations describing microphysical processes; these parameters are listed in Table 1. For each parameter, a minimum and maximum realistic value is defined as well as a `truth' value. When the model is integrated using this choice of parameters, the results are considered the synthetic true state of the atmosphere, and simulated observations of this model state are deemed observational truth (this is represented in gray in the schematic shown in Figure 2). As with real observations, the simulated observation is stochastic, and can be defined by a PDF. Assuming a Gaussian distribution for the observational uncertainty, this PDF is defined by two quantities { the mean, or _rst moment, and the covariance, or second moment. The observational truth is used to define the mean, implying unbiased observations. The observations were assigned a multi level error covariance which was simulated explicitly from a large Monte Carlo ensemble that

was based on Posselt and Vukicevic (2010) simulations. The choice of the microphysical parameters of interest defines a ten-dimensional control parameter space. This space is explored so as to determine the ten-dimensional probability density function of the parameters conditioned on information in the observations.

TABLE 1. Cloud microphysical parameter descriptions, abbreviation, along with truth values and parameter ranges. Table reproduced from PV10.

Parameter description	Abbreviation	Units	Truth	Min	Max
Snow fall speed coefficient	a_s	cm^{1-b_s}	200.0	50.0	1000.0
Snow fall speed exponent	b_s	none	0.3	0.1	1.0
Graupel fall speed coefficient	a_g	cm^{1-b_g}	400.0	50.0	1200.0
Graupel fall speed exponent	b_g	none	0.4	0.1	0.9
Intercept parameter of the rain particle size distribution	N_{0r}	cm^{-4}	0.5	0.0	5.0
Intercept parameter of the snow particle size distribution	N_{0s}	cm^{-4}	0.5	0.0	5.0
Intercept parameter of the graupel particle size distribution	N_{0g}	cm^{-4}	0.5	0.0	5.0
Snow particle density	ρ_s	g cm^{-3}	0.2	0.1	1.0
Graupel particle density	ρ_g	g cm^{-3}	0.4	0.1	1.0
Threshold cloud mass mixing ratio for autoconversion to rain	q_{c0}	g kg^{-1}	1.0	0.1	3.0

Although only microphysical parameters were directly perturbed, all model variables and simulated observations affected by these perturbations are also described by a probability density function under the constraints of the model-observational system. In the results the ten-dimensional parameter PDFs are presented as well as joint PDFs of parameters and observations, parameters and microphysical process activity, and microphysical process activity PDFs. The ten-dimensional posterior microphysical parameter PDF represent the solution to the inverse problem and provides robust estimates of uncertainty in the parameters when constrained by the radar reflectivity observations. In order to illuminate observational constraint in the data assimilation which results from the relationship between parameters and observations by the models, posterior PDFs of the joint parameter-observation space are then analyzed. These PDFs show the sensitivity of radar reflectivity simulated observations to simultaneous perturbation of microphysical parameters; in addition, they illustrate which vertical levels provide observational constraint to each parameter. Then, in order to determine why observations are sensitive to perturbations in microphysical parameters, joint PDFs of microphysical parameters and activity of individual microphysical processes within the parameterization scheme are evaluated. The microphysical processes included in this analyses are listed in Table 2. The

process-activity PDFs demonstrate the actual microphysical response to simultaneous perturbation of the ten microphysical parameters and yield insight into how parameter perturbation affects modeled cloud microphysics. From these, the conclusions are finally derived about the approach to stochastic modeling of the processes by controlling the processes directly and not by the choice of physical parameters. These conclusions present basis for the next and final phase of the project.

TABLE 3. Microphysical process descriptions, abbreviation, source and product hydrometeors of the process. Note that ERN, the evaporation of rain, is a negative definite quantity and here only the absolute value is shown.

Process description	Abbreviation	Source	Product
Evaporation of rain (negative)	ERN	Rain	Water Vapor
Melting of snow	PSMLT	Snow	Rain
Melting of graupel	PGMLT	Graupel	Rain
Cloud ice accretion of rain	PIACR	Cloud Ice, Rain	Snow, Graupel
Graupel accretion of rain	DGACR	Graupel, Rain	Graupel
Snow accretion of rain	PSACR	Rain, Snow	Snow, Graupel
Autoconversion of cloud water to rain	PRAUT	Cloud water	Rain
Rain accretion of cloud water	PRACW	Rain, Cloud water	Rain
Graupel accretion of cloud water to produce rain	QGACW	Graupel, Cloud water	Rain
Rain accretion of snow	QRACS	Rain, Snow	Rain
Deposition on snow	PGDEP	Water Vapor,Snow	Snow
Snow accretion of cloud water	PSACW	Cloud water, Snow	Snow, Graupel
Bergeron process (deposition/riming)	PSFW	Cloud water	Snow
Deposition on graupel	PGDEP	Water vapor	Graupel
Graupel accretion of cloud water	DGACW	Graupel, Cloud water	Graupel

1b) Major findings of the study on quantifcation of cloud microphysical parameterization uncertainty using radar reflectivity

Radar reflectivity observations are shown to more tightly constrain microphysical parameter uncertainty than the column-integral observations used in Posselt and Vukicevic (2010) { reducing variance and in some cases eliminating biases in the parameter inversion. In particular, ice fall speed parameters and intercept parameters of hydrometeor particle size distribution are shown to be considerably better constrained by radar reflectivity observations (Figure 2). Non-uniqueness shown by PV10 in the inverse solution for ice hydrometeor fall speed parameters is eliminated with the use of radar reflectivity, although the posterior PDF for cloud water-to-rain auto-conversion threshold shows a

bimodal structure which was not observed in PV10 for column-integral observations { a sign of non-uniqueness in the inverse solution. This property is a likely consequence of microphysical processes which serve to compensate for modified hydrometeor concentration associated with the spurious mode of this parameter. These results demonstrate the increased information content of radar reflectivity relative to column-integral measurements as well as the utility of the probabilistic analyses employed.

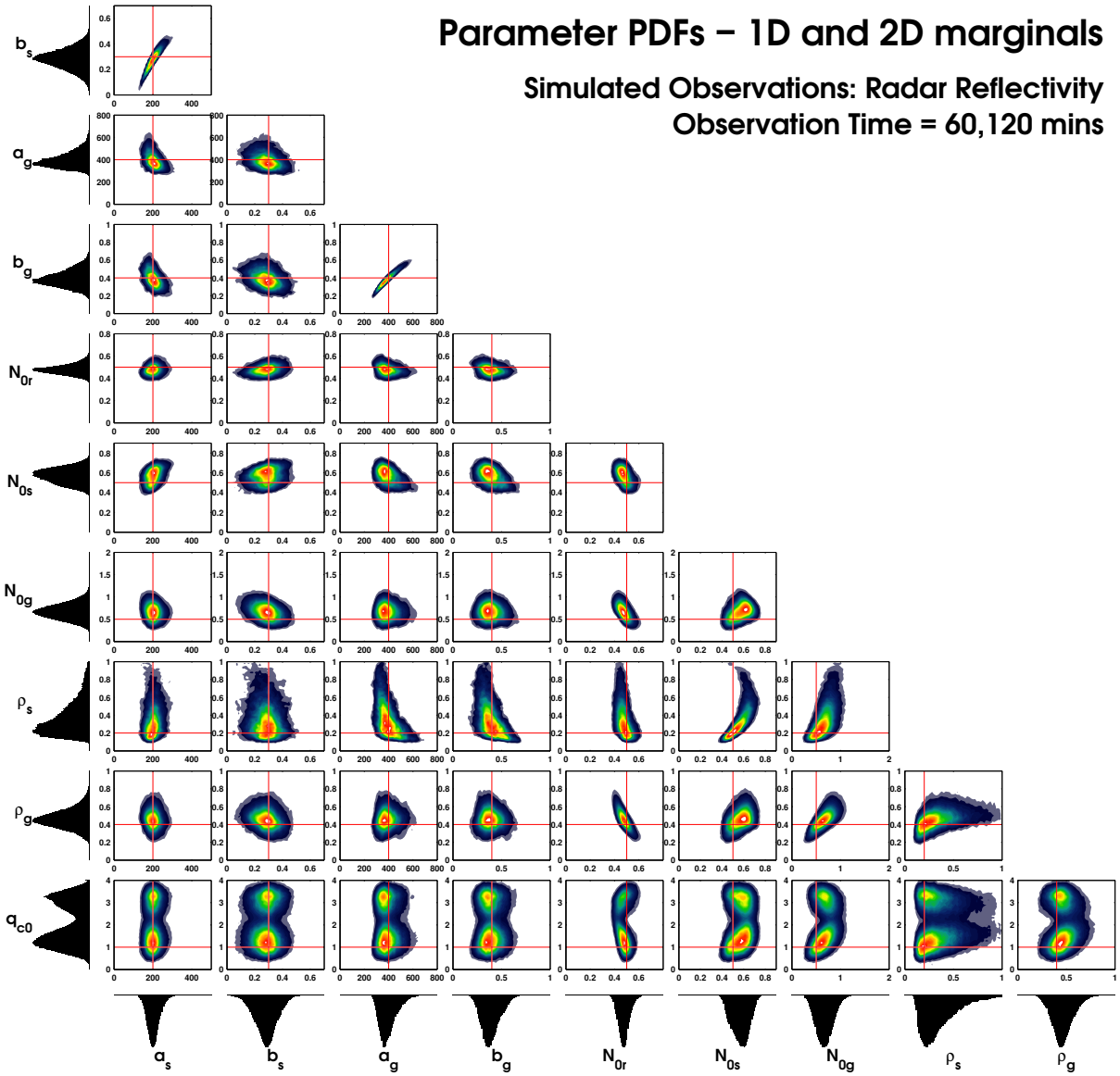

Figure 2: 1D Lagrangian model simulation of rain mixing ratio (kg/kg)

Interpretation of microphysical parameter uncertainty under the constraint of radar reflectivity is then facilitated by a number of novel analyses. Joint parameter-observation

PDFs allow for a diagnosis of what observational levels constrain parameter uncertainty. It is found that in many cases, these relationships yield to intuitive analysis, while in other cases, sensitivity of observation to parameter perturbation is likely the product of complex microphysical interactions (Figure 3). For example, evaporation of rain, graupel accretion of rain, and rain accretion of cloud water are shown to change the sign of their first order relationship with all parameters between the stratiform and convective storm regimes. These analyses also underscore the value of a vertically resolved observable quantity { in many cases the relationship between reflectivity and parameter perturbation is strongly height-dependent.

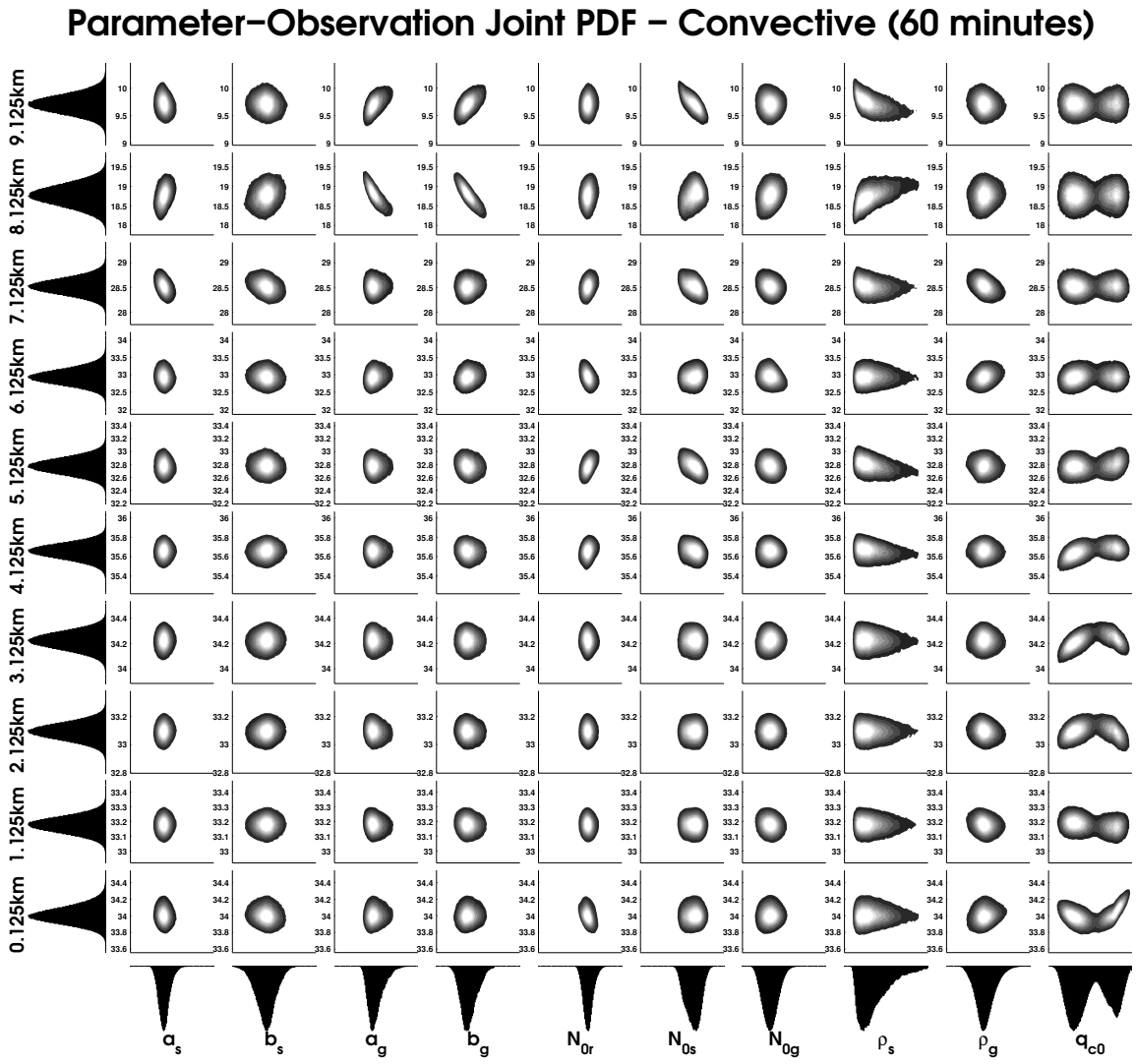

Figure 3A: Joint PDF of parameter and radar reflectivity observations at various vertical for a time **during convective** phase of simulated squall-line. Each row corresponds to simulated reflectivity at a particular model level, whereas each column corresponds to a different model physics

parameter.

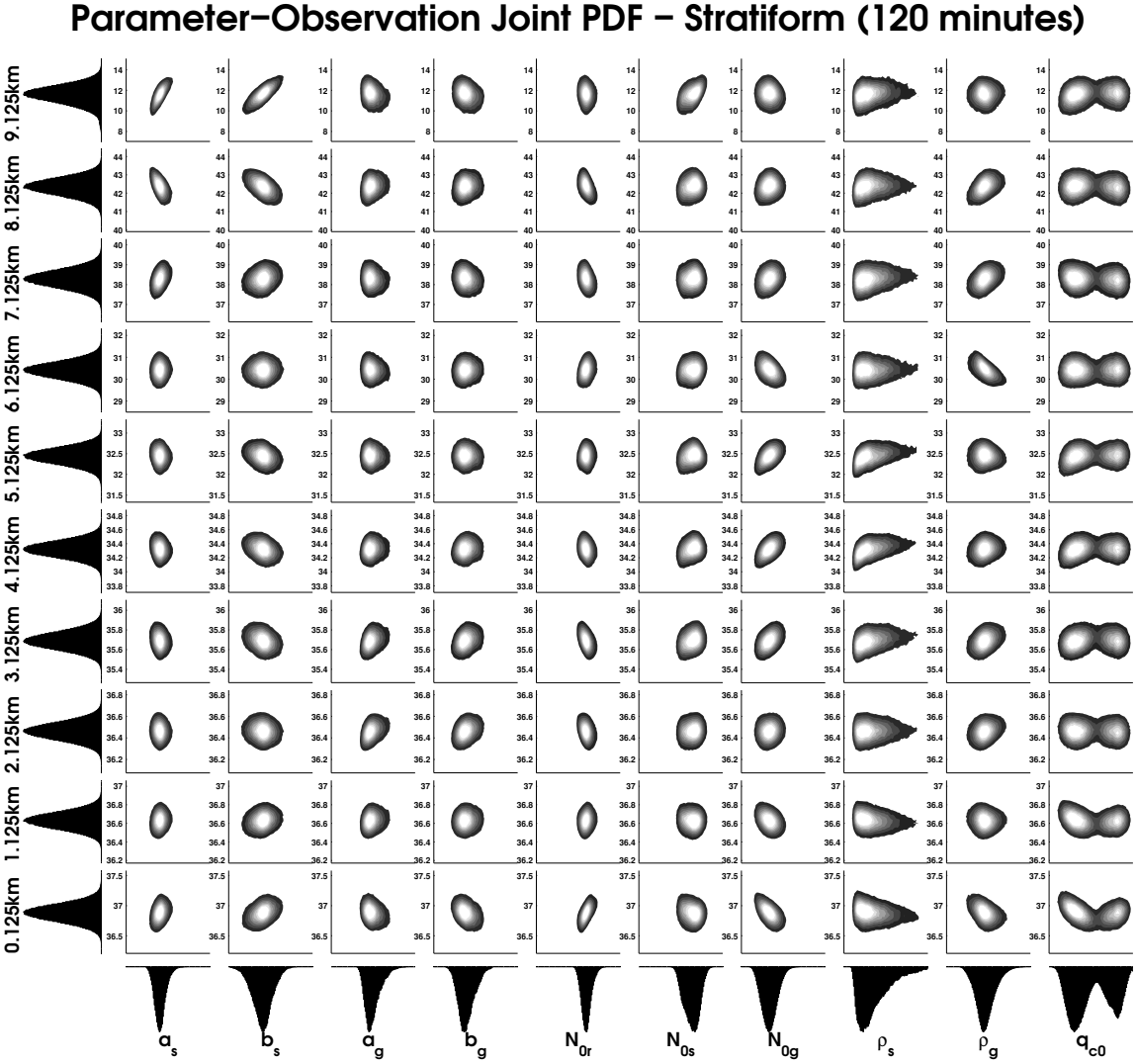

Figure 3B: Joint PDF of parameter and radar reflectivity observations at various vertical for a time **during stratiform** phase of simulated squall-line. Each row corresponds to simulated reflectivity at a particular model level, whereas each column corresponds to a different model physics parameter.

Finally, PDFs of microphysical process activity are produced in order to further analyze the processes which contribute to the microphysical state, and thus, the observable state of the model. The activity of a number of microphysical processes are integrated over times in the convective and stratiform regimes and treated probabilistically. The results show that the behavior of microphysical processes and the relationship between uncertainty in parameters and microphysical processes is strongly dependent on storm

morphology. For example, the relationship between graupel accretion of cloud water and rain accretion of cloud water changes its sign between convective and stratiform storm regimes. This is an indication that in different storm morphological regimes, distinct microphysical processes and hydrometeor types may provide the primary constraint on microphysical behavior (Figure 4).

The PDF, fully in process space, allows for observation of the interrelationships between microphysical processes.(Figure 5). The shape of these distributions (the number of modes, skewness and linearity of interrelationships) provides insight into the ease with which microphysical uncertainty might be represented in a parameterization scheme. Specifically, the greater the degree to which the PDF resembles a multivariate Gaussian distribution, the easier this uncertainty might be stochastically reproduced. The current results show that microphysical process PDFs appear to be somewhat more “well behaved" than parameter PDFs,.This suggests that a stochastic representation of microphysical processes may more closely describe microphysical parameterization uncertainty than a stochastic representation of microphysical parameters. In the current study, however, microphysical process PDFs are limited by the fact that it is parameters, and not processes, which are directly perturbed.

In the next study we will investigate inversions with individual as well as multiple microphysical processes as control parameters using MCMC experiments. The results would be then related relate to the more practical data assimilation approaches such as 4DVAR and Ensemble Kalman Filter, by evaluation of maximum likelihood, mean and covariance solutions that would be derived from the full PDF solutions.

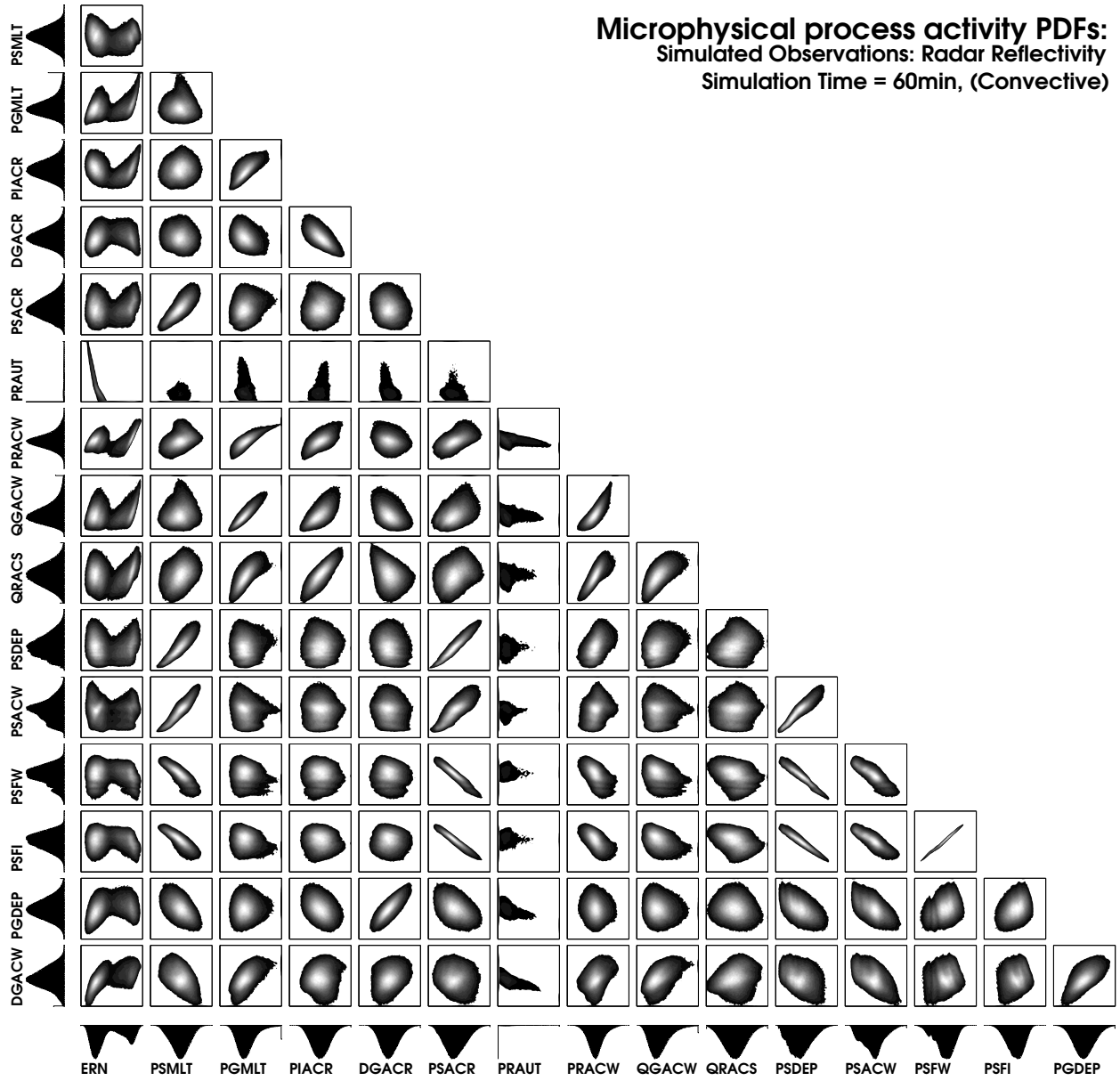

Figure 5A: Joint PDF of microphysical process activity during the convective phase of the squall-line development (40-80 minutes)

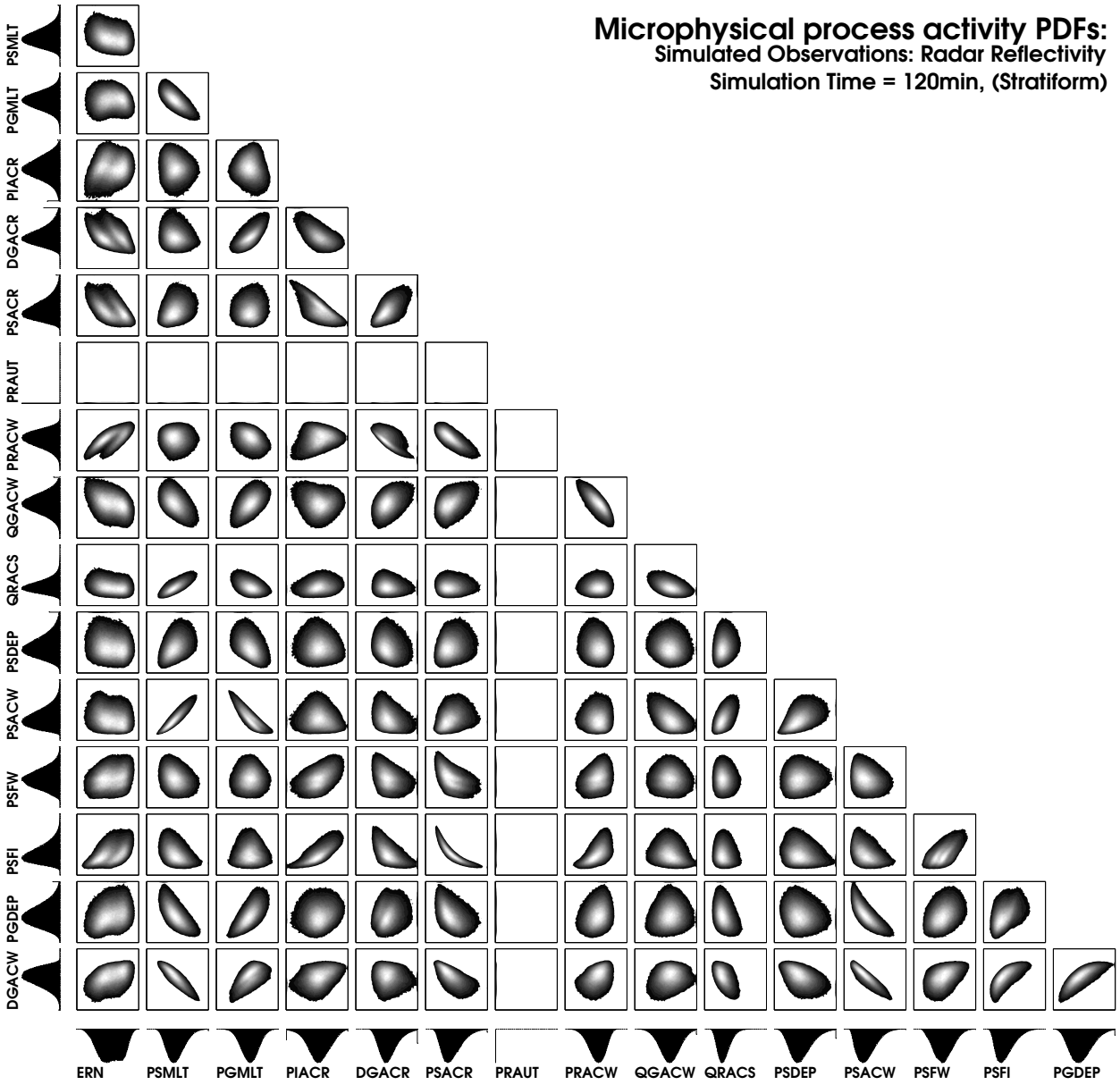

Figure 5B: As in 5A but for microphysical process activity during the stratiform phase of the squall-line development (100-140 minutes)

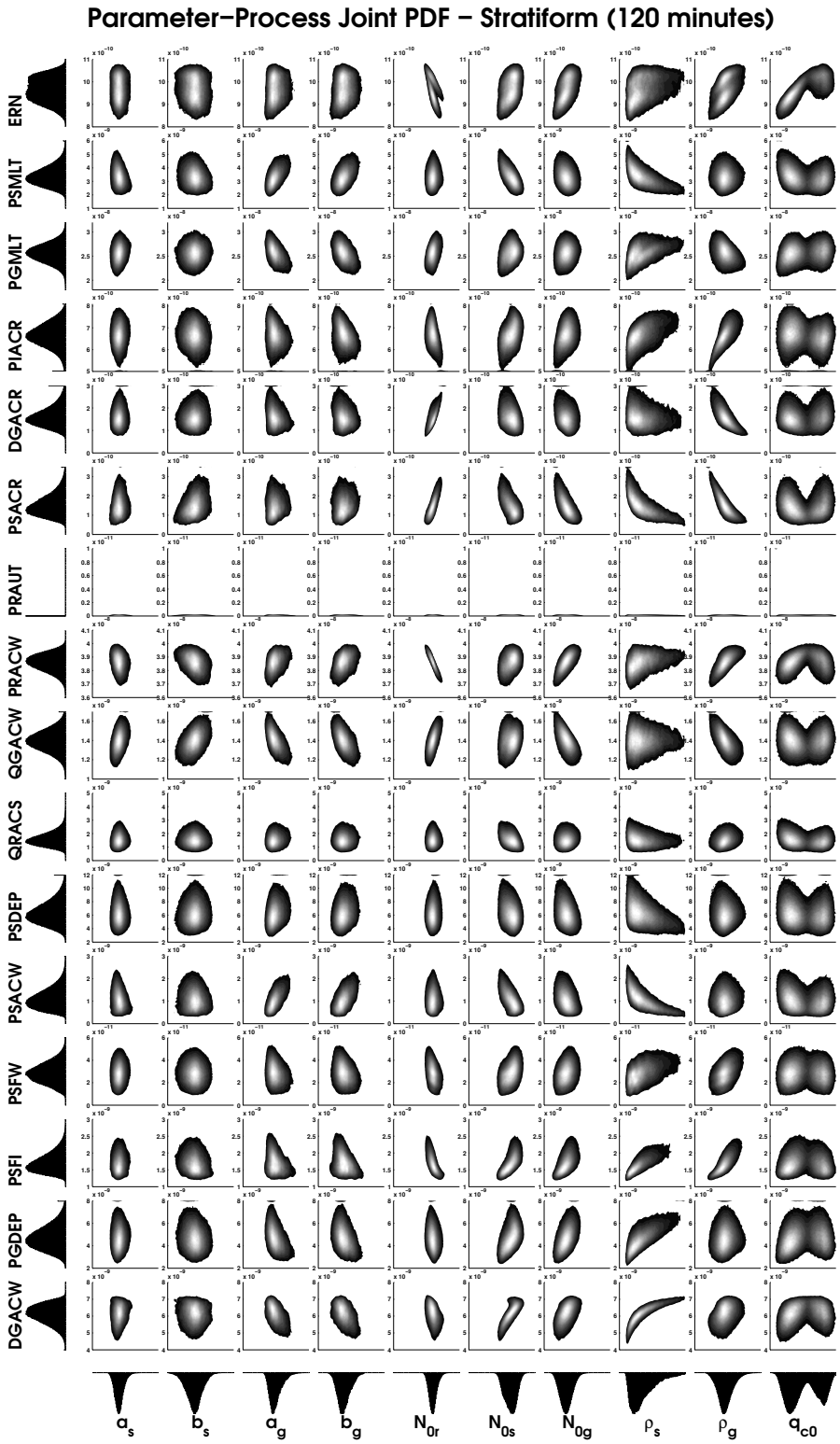

Figure 4 A: Joint PDF of parameters and microphysical process activity during convective phase of squall-line development. Each row represents a spatio-temporal integral of process activity while each column represents a microphysical parameter.

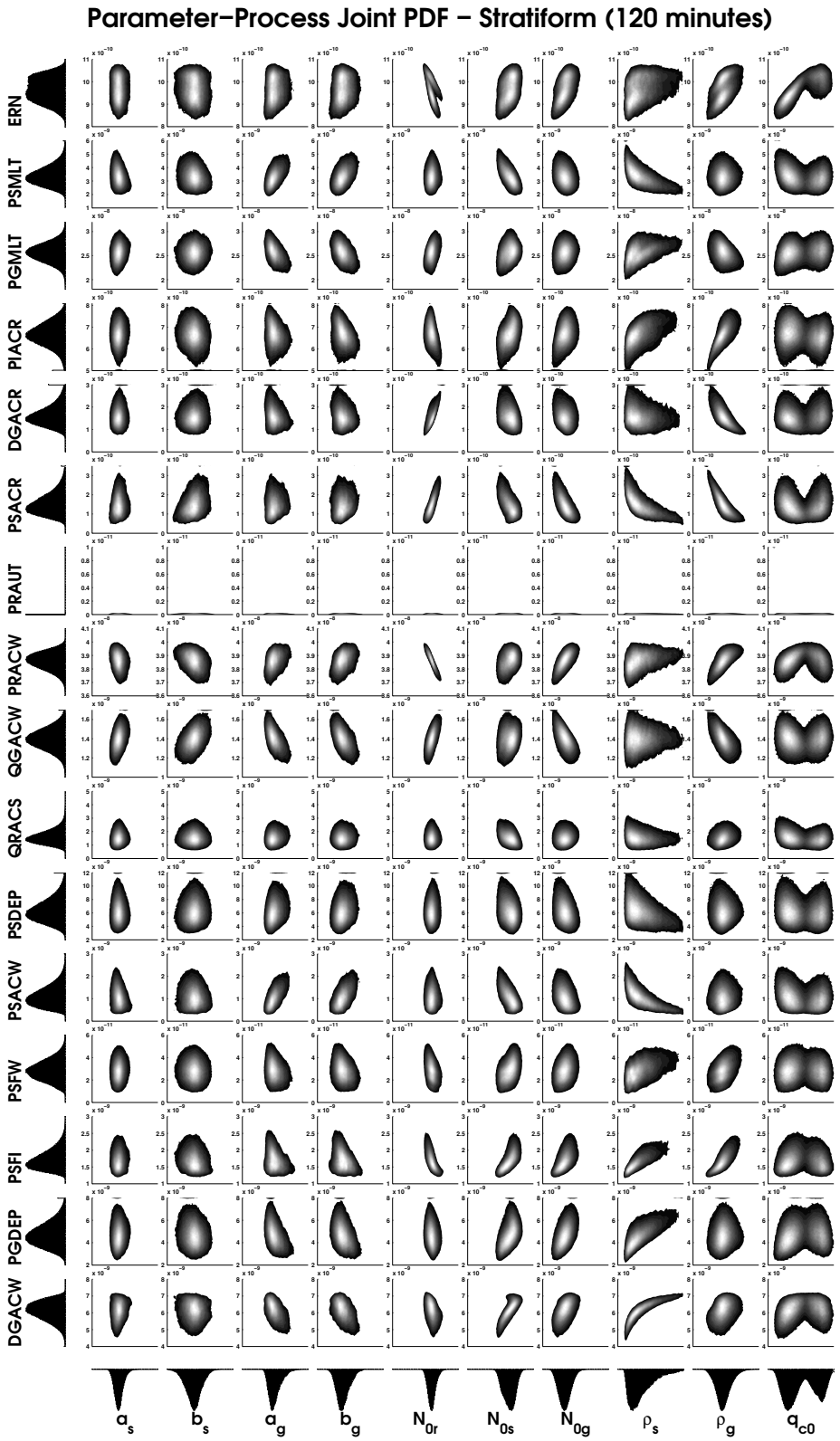

Figure 4 B: As in4A but for process activity during stratiform phase of squall-line development.